

Finite-Element Methods for the Calculation of Capillary Surfaces

ROBERT A. BROWN

*Department of Chemical Engineering and Materials Science,
University of Minnesota, Minneapolis, Minnesota 55455*

Received August 4, 1978; revised December 28, 1978

Galerkin finite-element methods of high accuracy are developed for solving the capillary equation, the nonlinear elliptic partial differential equation describing the shape of an interface between two immiscible fluids. The calculation of an interface meeting the walls of a capillary of square cross section at a given contact angle is used as a model problem in numerical experiments comparing the relative efficiencies of bilinear, reduced quadratic, biquadratic, and Hermite bicubic finite-element interface approximations. Newton methods are employed for solving the nonlinear algebraic equation sets resulting from the finite-element discretizations. The Hermite bicubic element is the most efficient because of the relatively few number of elements needed to calculate highly accurate interface shapes. The reduced quadratic finite-element-Newton method is also tested against a finite-difference scheme. The finite-element calculations are demonstrated more efficient.

1. INTRODUCTION

The shape of an interface between two immiscible static fluids is described by the well-known Young-Laplace or capillary equation which proportionates the local mean curvature of the interface to the drop in static pressure across it. Once a spatial coordinate representation for the interface has been assumed, the capillary equation is readily seen as a nonlinear elliptic partial differential equation in two space dimensions. Closed-form solutions of the full capillary equation are rare and the computer has been enlisted to generate approximate interface shapes.

A numerical algorithm for the solution of the capillary equation or any nonlinear elliptic differential equation can be characterized by the discretization used to approximate the equation's solution and the iteration technique used to solve the resulting set of nonlinear equations. Finite-difference methods are traditionally used for discretization. Finite-element methods are gaining popularity. Methods for solving nonlinear equations such as Newton's method, secant method, and successive approximations yield linear equation sets at each iteration and can be further classified by the technique, either direct or iterative, that is used to solve the system of equations.

Both finite-difference [1-4] and finite-element [4-10] methods have been used for approximating the capillary equation. These approximations and the nonlinear iteration methods used with them are summarized in Table I. In this report we detail a finite-element-Newton method for the numerical solution of the capillary equation.

TABLE I
Previous numerical solutions of the capillary equation.^a

Work	Type of approximation	Nonlinear iteration technique	Linear equation solver
Larkin [1]	Finite difference	Explicit marching in 1 direction	Direct factorization of tridiagonal matrix
Orr <i>et al.</i> [4]	Finite difference	Full Newton method	Successive overrelaxation
Doss [3]	9-point finite difference, see [11]	Successive approximations	Dynamic alternating direction implicit method
Concus <i>et al.</i> [2]	9-point finite difference, see [11]	Successive approximations	Nonlinear conjugate gradient method
Orr <i>et al.</i> [4, 5]	Linear finite elements on triangles	Successive approximations	Direct factorization
Mittelmann [6]	Linear finite elements on triangles	Full Newton method	Successive overrelaxation
Albright [7]	Bilinear finite elements on quadrilaterals	Full Newton method	Block successive overrelaxation
Silliman, Scriven [8]	Linear finite elements on triangles	Full Newton method	Direct factorization
Brown <i>et al.</i> [9], Brown [10]	Reduced quadratic finite elements on quadrilaterals	Full Newton method	Direct factorization
This work	Bilinear, reduced quadratic, biquadratic, and Hermite bicubic finite elements on quadrilaterals	Full, simple, and adaptive Newton methods	Direct factorization

^a Each technique is catalogued according to the approximation used for the capillary interface and the iteration method used for solving the resulting nonlinear equation set.

The method differs from earlier finite-element approximations to this problem [4-8] in that here reduced quadratic, biquadratic, and Hermite bicubic finite-element basis functions of higher-order accuracy are used instead of the more easily formulated linear approximation.

Three variants of Newton's method are tested for solution of the nonlinear finite-element equations: (1) the standard Newton procedure where the Jacobian matrix \mathbf{J} is formulated at each iteration, (2) simplified Newton iteration in which \mathbf{J} is calculated only initially, and (3) an adaptive method that combines the desirable features of both (1) and (2). Direct factorization is used to solve the linear equation sets that result at each iteration in all three methods.

Since few convergence estimates for numerical solution of the capillary problem are known, empirical estimates must be inferred from computational experiments. The high-order finite-element approximations are compared with a similar finite-element formulation using bilinear basis functions and also to the finite-difference approximation of Concus [11] as implemented by Doss [3]. The model capillary problem used as the basis of these comparisons is the calculation of the shape of the interface between two immiscible fluids in a square capillary. Here the sides of the capillary are coordinate surfaces and both finite-difference and finite-element discretizations are easily computed, although the finite-element methodology extends to capillaries with irregular shapes where it has clear advantages over finite-difference methods [10]. The model problem has been chosen because it admits a simple closed-form solution; when the effects of gravity are unimportant, the interface shape is given by a piece of sphere. This known solution allows comparisons of accuracy for numerical approximations.

The finite-element-Newton algorithm presented here is not limited to the capillary problem, but is applicable for any nonlinear elliptic partial differential equation in divergence form [12, 13].

2. THE CAPILLARY PROBLEM

The Young-Laplace or capillary equation is simply written as

$$2H\sigma = p_A - p_B = \Delta p, \quad (1)$$

where σ is the interfacial tension of the interface, H is the local mean curvature, and Δp is the drop in pressure across the interface (see Fig. 1). For an interface whose elevation can be represented in rectangular cartesian coordinates $u = u(x, y)$, the mean curvature of the interface is given as

$$2H \equiv -\nabla_{\text{II}} \cdot \mathbf{N} = -\nabla_{\text{II}} \cdot \frac{\mathbf{k} - u_x \mathbf{i} - u_y \mathbf{j}}{(1 + u_x^2 + u_y^2)^{1/2}}, \quad (2)$$

\mathbf{N} is the unit vector field everywhere normal to the interface, $\nabla_{\text{II}} = \mathbf{i}\partial/\partial x + \mathbf{j}\partial/\partial y$,

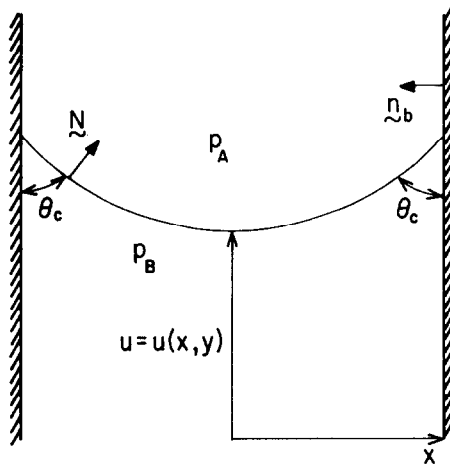


FIG. 1. Vertical cross section of interface between two immiscible static fluids in a square capillary. The interface meets the capillary's walls at a prescribed contact angle θ_c .

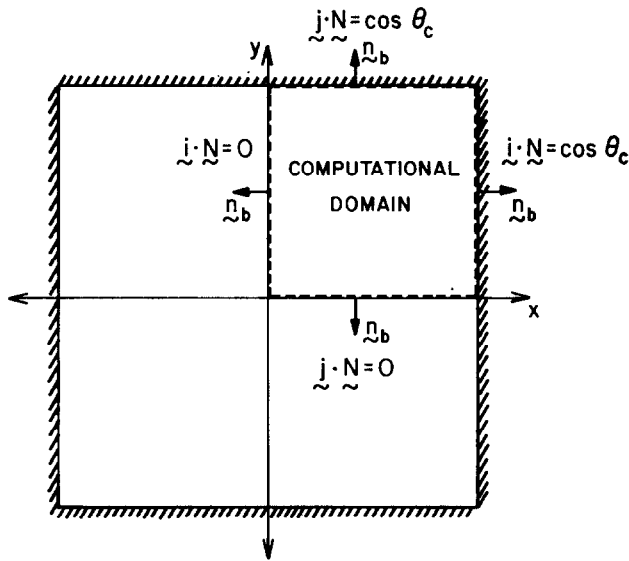


FIG. 2. Computational domain for the calculation of an interface in a square capillary. Symmetry and capillary wall boundaries are shown.

and (i, j, k) are the unit vectors in the (x, y, u) directions. Substituting (2) into (1) gives

$$-\nabla_{II} \cdot N = \Delta p / \sigma \equiv K \tag{3}$$

or

$$\frac{(1 + u_y^2) u_{xx} - 2u_x u_y u_{xy} + (1 + u_x^2) u_{yy}}{(1 + u_x^2 + u_y^2)^{3/2}} = K. \tag{4}$$

As shown in Fig. 2, the square capillary geometry has two planes of reflective symmetry and the computational domain is taken as only one quadrant of the capillary's entire cross section. The boundary conditions for (2) or (3) are prescribed at the symmetry boundaries $\partial\mathcal{D}_{\text{SYM}}$ and the capillary's walls $\partial\mathcal{D}_{\text{SOLID}}$. Along $\partial\mathcal{D}_{\text{SOLID}}$ the interface meets the capillary at a prescribed contact angle θ_c which is defined in terms of \mathbf{n}_b , the outward directed unit normal to the wall as

$$\mathbf{N} \cdot \mathbf{n}_b = \cos \theta_c, \quad \text{on } \partial\mathcal{D}_{\text{SOLID}}. \tag{5}$$

On $\partial\mathcal{D}_{\text{SYM}}$ the symmetry boundary condition is

$$\mathbf{N} \cdot \mathbf{n}_b = 0, \quad \text{on } \partial\mathcal{D}_{\text{SYM}}. \tag{6}$$

When the pressure difference K is taken as a constant, Eq. (4) describes a surface of constant mean curvature $\frac{1}{2}K$ and a simple solution of (4)–(6) is known. For $45^\circ \leq \theta_c \leq 90^\circ$ the piece of sphere

$$u^E(x, y) = 1/\cos \theta_c - [1/\cos^2 \theta_c - x^2 - y^2]^{1/2} \tag{7}$$

gives an equilibrium interface shape if

$$K = \frac{4 \cos \theta_c}{D}; \tag{8}$$

where D is the side length of the capillary. Equation (8) is a necessary constraint for equilibrium that arises from the balance of vertical forces (constructed by integrating Eq. (3) over \mathcal{D}) on the interface.

Concus and Finn [14] have shown that for $\theta_c < 45^\circ$ the solution to Eqs. (4)–(6) fails to exist in the neighborhood of the corner. Physically, for $\theta_c < 45^\circ$, a film of liquid will run up the corner. The film will rise past the point where its thickness is smaller than that allowed for a bulk liquid phase and Eq. (4) becomes invalid.

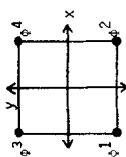
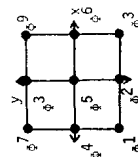
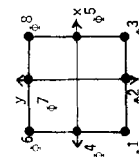
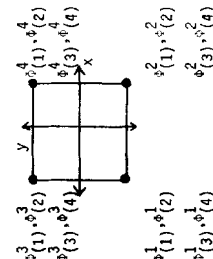
3. GALERKIN FINITE-ELEMENT METHOD

The Galerkin finite-element method as previously presented in [5–11] is implemented to approximate the solution of the capillary equation (3) and the boundary conditions (5) and (6). The computational domain is divided into quadrilateral subdomains or elements on which a set of polynomial basis or trial functions is defined. The interface shape $u(x, y)$ is approximated in each element E as a sum of these basis functions multiplied by unknown coefficients

$$u(x, y) = \sum_{\substack{\text{all } i \\ \text{in } E}} \alpha_i \Phi^i(x, y) \quad \text{in } E. \tag{9}$$

The bilinear, reduced quadratic, biquadratic, and Hermite bicubic polynomial basis functions studied in this report are summarized in Table II.

TABLE II
Finite-element basis functions.

Element	Schematic	Basis functions	Number of unknowns \mathcal{N}	Predicted error $\ u - u^E\ _2$	Continuity
Bilinear		$\Phi^i(x, y) = a_1^i + a_2^i x + a_3^i y + a_4^i xy$ $\Phi^i(x_j, y_j) = \delta_{ij}, \quad i, j = 1, \dots, 4$	$M^2 + 2M + 1$	$\mathcal{O}(h^2)$	C^0
Biquadratic		$\Phi^i(x, y) = a_1^i + a_2^i x + a_3^i y + a_4^i xy$ $+ a_5^i x^2 + a_6^i y^2 + a_7^i x^2 y$ $+ a_8^i x y^2 + a_9^i x^2 y^2$ $\Phi^i(x_j, y_j) = \delta_{ij}, \quad i, j = 1, \dots, 9$	$4M^2 + 4M + 1$	$\mathcal{O}(h^3)$	C^0
Reduced quadratic		$\Phi^i(x, y) = a_1^i + a_2^i x + a_3^i y + a_4^i xy$ $+ a_5^i x^2 + a_6^i y^2 + a_7^i x^2 y$ $+ a_8^i x y^2$ $\Phi^i(x_j, y_j) = \delta_{ij}, \quad i, j = 1, \dots, 8$	$3M^2 + 4M + 1$	$\mathcal{O}(h^3)$	C^0
Hermite bicubic		$\Phi_{(1)}^i = \Psi^i(x)\Psi^i(y), \quad \Phi_{(3)}^i = \Gamma^i(x)\Psi^i(y)$ $\Phi_{(3)}^i = \Psi^i(x)\Gamma^i(y), \quad \Phi_{(4)}^i = \Gamma^i(x)\Gamma^i(y)$ $\Psi^i(x) = a_1^i + a_2^i x + a_3^i x^2 + a_4^i x^3$ $\Psi^i(x_j) = \delta_{ij}, \quad d\Psi^i(x_j)/dx = 0, \quad i, j = 1, 2$ $\Gamma^i(x) = a_5^i + a_6^i x + a_7^i x^2 + a_8^i x^3$ $\Gamma^i(x_j) = 0, \quad d\Gamma^i(x_j)/dx = \delta_{ij}, \quad i, j = 1, 2$	$4M^2 + 8M + 4$	$\mathcal{O}(h^4)$	C^1

^a Accuracy predicted for solving Laplace's equation $\nabla^2 u = 0$.

The constants in the bilinear, reduced quadratic, and biquadratic polynomials are completely determined by the Lagrangian interpolation conditions specified at the element's nodes. The reduced quadratic element differs in form from the full biquadratic approximation only by the elimination of the x^2y^2 term from the polynomial and the omission of the centroid node from the element. The number of unknowns in each approximation for a $M \times M$ mesh of quadrilaterals of side length h is also shown in Table II along with the order of accuracy predicted for solving the linear Laplace's equation [15]. As is expected, the quadratic basis functions form more accurate solutions than the bilinear polynomials. They also have more unknowns $\{\alpha_i\}$ in their approximation for the same quadrilateral discretization of the domain.

These three Lagrangian basis functions lead to numerical solutions which are mathematically continuous everywhere in the domain \mathcal{D} but which have discontinuous first derivatives along element boundaries. The Hermite bicubic approximation also shown in Table II has by construction continuous first derivatives throughout \mathcal{D} and is of higher-order accuracy than either the quadratic or bilinear elements. More detailed accounts of these elements can be found elsewhere [15].

The coefficients $\{\alpha_i\}$ are determined by forcing the set of Galerkin weighted residual equations formed from Eq. (3) to zero, i.e.,

$$\int_{\mathcal{D}} \Phi_{(E)}^i (\nabla_{II} \cdot \mathbf{N} + K) da = 0, \quad i = 1, \dots, \mathcal{N}, \quad (10)$$

where \mathcal{N} is the total number of basis functions in the domain. Integrating Eq. (10) by parts and applying the divergence theorem gives

$$\int_{\mathcal{D}} (\Phi_{(E)}^i K - \nabla \Phi_{(E)}^i \cdot \mathbf{N}) da + \int_{\partial \mathcal{D}_{\text{SYM}}} \Phi_{(E)}^i \mathbf{n}_b \cdot \mathbf{N} ds + \int_{\partial \mathcal{D}_{\text{SOLID}}} \Phi_{(E)}^i \mathbf{n}_b \cdot \mathbf{N} ds = 0, \quad i = 1, \dots, \mathcal{N}. \quad (11)$$

Substituting the boundary conditions (5) and (6) into the residual Eqs. (11) yields

$$R^i(\alpha) = \int_{\mathcal{D}} (\Phi_{(E)}^i K - \nabla \Phi_{(E)}^i \cdot \mathbf{N}) da + \cos \theta_c \oint_{\partial \mathcal{D}_{\text{SOLID}}} \Phi_{(E)}^i(x, y) ds = 0, \quad i = 1, \dots, \mathcal{N}. \quad (12)$$

It is not merely fortuitous that the boundary conditions blend easily into the Galerkin residuals. These boundary conditions are the natural conditions for Eq. (3); Eq. (12) is the same result as obtained from a variational or energy minimization formulation of the capillary problem (see [6]).

Substituting the definition of \mathbf{N} given in Eq. (2) into Eq. (12) yields

$$R^i(\alpha) = \int_{\mathcal{D}} \left\{ \Phi_{(E)}^i K + \frac{\Phi_{(E)}^i u_x u_x + \Phi_{(E)}^i u_y u_y}{(1 + u_x^2 + u_y^2)^{1/2}} \right\} da + \cos \theta_c \oint_{\partial \mathcal{D}_{\text{SOLID}}} \Phi_{(E)}^i ds = 0, \quad i = 1, \dots, \mathcal{N}, \quad (13)$$

which, once the solution expansion Eq. (9) is introduced, is recognized as a nonlinear

algebraic equation set for $\{\alpha_i\}$. The area integrals in Eq. (13) are evaluated by Gaussian quadrature [17]. The four-point formula is used with bilinear and reduced quadratic basis functions, while the nine-point formula is necessary for calculations with Hermite bicubic elements. Biquadratic basis functions require the nine-point integration formula to ensure definiteness of the approximate residual equations (see [15, p. 189]).

4. SOLUTION OF FINITE-ELEMENT EQUATIONS

Because the set of residual equations (13) is nonlinear, its solution requires iteration. Many techniques are available, see [16] for a useful compendium. The three methods which are tested here are full Newton, simplified Newton, and adaptive Newton iterations. The differences between them are explained below.

The full Newton method (FNM) calculates the new $(k + 1)$ st iterate for the unknowns $\{\alpha_i^{(k+1)}\}$ by the formula

$$\alpha^{(k+1)} = \alpha^{(k)} - \mathbf{J}^{-1}(\alpha^{(k)})\mathbf{R}(\alpha^{(k)}) \equiv \alpha^{(k)} - \delta^{(k)}, \quad (14)$$

where the Jacobian matrix ($J_{ij} = \partial R^i / \partial \alpha_j$) is the local gradient of the residuals with respect to the unknown coefficients. This iteration is continued until the correction vector $\delta^{(k)}$ satisfies the convergence criterion

$$\|\delta^{(k)}\|_\infty = \max_{i=1, \dots, \mathcal{N}} |\delta_i^{(k)}| < \Delta e, \quad (15)$$

where Δe is a prescribed tolerance (usually 10^{-10}). At each iteration Eq. (14) requires the formulation and solution of the linear equation set

$$\mathbf{J}^{(k)} \delta^{(k)} = \mathbf{R}^{(k)} \quad (16)$$

with

$$J_{ij}(\alpha^{(k)}) = \int_{\mathcal{D}} \left\{ \frac{\Phi_{(E)x}^i \Phi_{(E)x}^j + \Phi_{(E)y}^i \Phi_{(E)y}^j}{(1 + u_x^2 + u_y^2)^{1/2}} - \frac{(\Phi_{(E)x}^i u_x + \Phi_{(E)y}^i u_y)(\Phi_{(E)x}^j u_x + \Phi_{(E)y}^j u_y)}{(1 + u_x^2 + u_y^2)^{3/2}} \right\}_{\alpha = \alpha^{(k)}} da. \quad (17)$$

The matrix \mathbf{J} is symmetric, sparse, and banded. The bandwidth depends on the numbering scheme for the nodes. Equation (16) is solved by factoring \mathbf{J} into \mathbf{LDL}^T form, where \mathbf{L} is lower triangular and \mathbf{D} is diagonal; this is done using profile matrix storage techniques as implemented in [17]. The resulting triangular equation systems are easily solved.

In the simple Newton method (SNM) the Jacobian matrix is formulated and factored only for the initial approximation $\{\alpha^{(0)}\}$. Successive iterates are calculated with this initial gradient approximation

$$\alpha^{(k+1)} = \alpha^{(k)} - \mathbf{J}^{-1}(\alpha^{(0)})\mathbf{R}(\alpha^{(k)}). \quad (18)$$

An iteration of SNM requires only the calculation of $\mathbf{R}(\alpha^{(k)})$ and the solution of the triangular systems

$$\mathbf{L}(\alpha^{(0)})\mathbf{D}(\alpha^{(0)})\mathbf{L}^T(\alpha^{(0)})\delta^{(k)} = \mathbf{R}(\alpha^{(k)}). \tag{19}$$

For mildly nonlinear equation sets SNM may be expected to be efficient. The accuracy of the updated gradient approximation in FNM leads to accelerated convergence, but at the expense of more computation, compared to SNM in which the gradient approximation is not updated.

Yet another alternative is an adaptive Newton method (ANM) which consists of an initial full Newton iteration followed by SNM iterations as long as the convergence rate $f^{(k+1)}$

$$f^{(k+1)} \equiv \|\delta^{(k+1)}\|_2 / \|\delta^{(k)}\|_2, \tag{20}$$

where $\|\delta^{(k)}\|_2^2 = \sum_{i=1}^N \delta_i^{(k)2}$, is smaller than a specified level f_0 ; the value $f_0 = \frac{1}{2}$ is employed here. If during execution $f^{(k+1)}$ increases above f_0 , a new approximation to the Jacobian matrix is calculated and factored, and the iterations are continued. The ANM iteration procedure is shown schematically in Fig. 3.

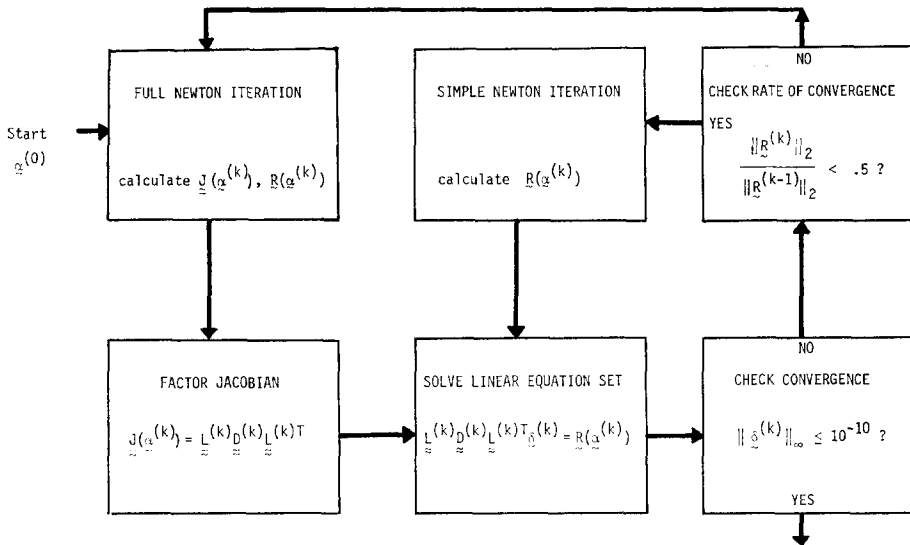


FIG. 3. Schematic of adaptive Newton method (ANM) algorithm. Full Newton (FNM) and simple Newton (SNM) schemes are produced by setting the convergence rate check to NO and YES, respectively.

The three iteration schemes, FNM, SNM, and ANM, for solving the nonlinear equation set (13) generated for the shape of an interface in a square capillary with contact angles of 80°, 60°, and 45° are compared in Tables III and IV. Grids of 8 and

16 reduced quadratic elements in each direction were employed in these calculations which were performed on the CDC Cyber 74 computer at the University of Minnesota. Timing estimates are reported in central processor seconds. The initial approximation $\{\alpha_i^{(0)}\}$ was taken to be a flat interface in all calculations.

TABLE III

Execution times for single iterations of full Newton (FNM) and simple Newton (SNM) methods.

	Time/iteration (cp sec)			
	8 × 8 grid		16 × 16 grid	
	FNM	SNM	FNM	SNM
Form $\mathbf{J}(\alpha^{(k)})$, $\mathbf{R}(\alpha^{(k)})$	0.33	—	1.37	—
Form $\mathbf{R}(\alpha^{(k)})$	—	0.14	—	0.54
Factor $\mathbf{J}(\alpha^{(k)})$	0.16	—	1.75	—
Solve Eq. (16)	0.03	—	0.21	—
Solve Eq. (19)	—	0.03	—	0.21
Total time	0.52	0.17	3.33	0.65

The execution times for single iterations of SNM and FNM are summarized in Table III. The SNM iteration is factors of 3 and 5 faster than the FNM iteration for 8×8 and 16×16 grids, respectively. The increase in this ratio with grid refinement is due to the increasing importance of the factorization of \mathbf{J} in the overall cost of a FNM iteration.

The results of the convergence tests for the three Newton methods are tabulated in Table IV. The number of iterations required for convergence of all three methods is insensitive to the number of elements used in the finite-element approximation. For $\theta_0 = 80^\circ$ the interface is nearly flat and ANM reduces in actuality to SNM; the initially calculated Jacobian matrix is a good approximation for later iterations and SNM converges quickly enough that the adaptive method need not update \mathbf{J} .

For contact angles of 60° and 45° , the initial Jacobian matrix is no longer a good approximation for later iterations; SNM converges very slowly and is less efficient than either FNM or ANM. For low contact angles ANM is as or more efficient than FNM. Its efficiency is due to its flexibility; it mimics the behavior of both SNM and FNM in the regions where these methods converge rapidly. No attempt has been made to optimize the convergence rate criterion f_0 ; better convergence may be obtained by specifying f_0 adaptively at each iteration.

TABLE IV

Comparison of full, simple, and adaptive Newton methods for reduced quadratic finite element calculation with contact angles of 80°, 60°, and 45°.

Iteration method	θ_c (deg)	8 × 8 GRID				16 × 16 GRID			
		Number of iterations		Execution Time (cp sec)	Number of iterations		Execution time (cp sec)		
		J recalculated	Old J used		J recalculated	Old J used			
SNM	80	1	9	1.0×10^{-10}	2.11	1	8	1.0×10^{-10}	10.05
ANM	80	1	9	1.0×10^{-10}	2.11	1	8	1.0×10^{-10}	10.05
FNM	80	4	0	1.0×10^{-10}	2.33	4	0	1.0×10^{-10}	14.20
SNM	60	1	40	1.0×10^{-10}	6.53	1	40	1.0×10^{-10}	33.57
ANM	60	3	8	1.0×10^{-10}	3.37	2	16	1.0×10^{-10}	19.33
FNM	60	6	0	1.0×10^{-10}	3.33	6	0	1.0×10^{-10}	20.38
SNM	45	1	40	1.8×10^{-8}	7.78	1	40	2.0×10^{-2}	34.62
ANM	45	5	10	1.0×10^{-10}	4.68	5	11	1.0×10^{-10}	28.54
FNM	45	9	0	1.0×10^{-10}	5.20	10	0	1.0×10^{-10}	33.50

5. COMPUTATIONAL EXPERIMENTS

Fortran computer programs implementing the four finite-element basis functions presented above have been written for the calculation of an interface in a square capillary with $D = 2$. Sample interface shapes for contact angles of 80° , 60° , 50° , and 45° are shown in Fig. 4. As θ_c is decreased from 90° , the interface shape becomes progressively steeper until at $\theta_c = 45^\circ$ the true gradient of the interface $|\nabla u^E|$ becomes infinite in the corner. Because the nonlinearity in (3) depends on the gradient $|\nabla u|$, interface shapes corresponding to contact angles near 45° are difficult to calculate;

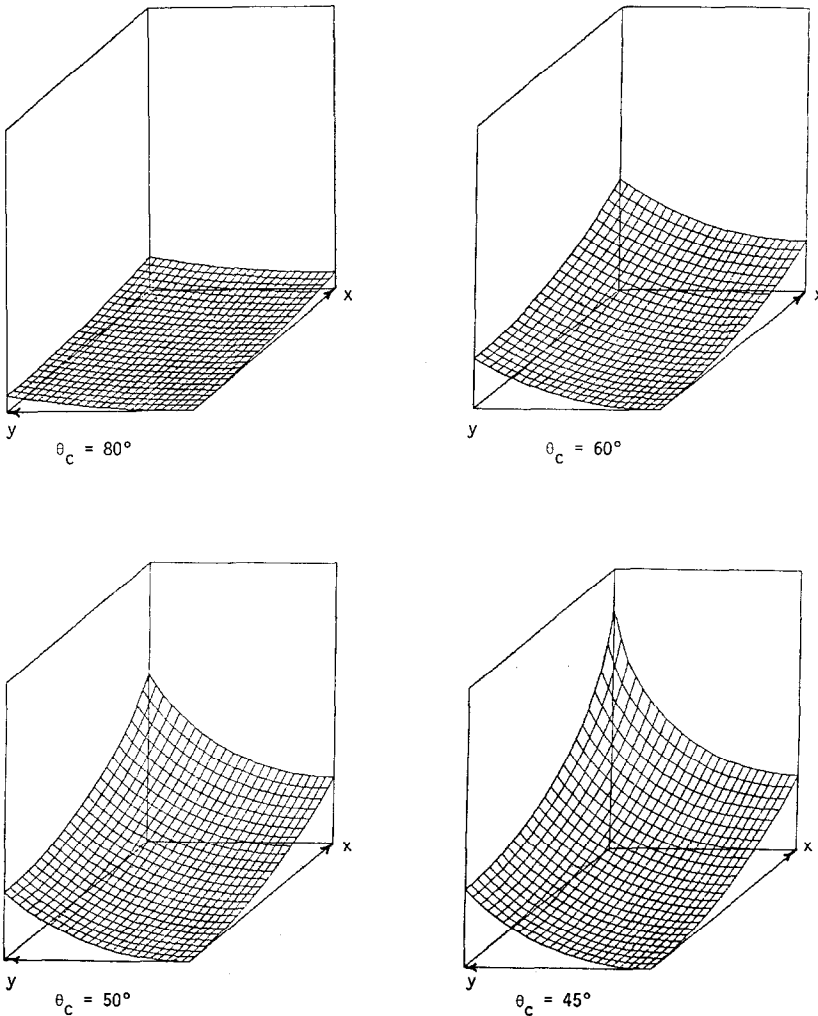


FIG. 4. Oblique views of capillary surfaces in one quadrant of a square capillary for $\theta_c = 80^\circ$, 60° , 50° , and 45° .

the convergence of the nonlinear iteration is slower and the calculated shapes have more error than those corresponding to higher contact angles.

The four finite-element approximations have been compared in these calculations according to their accuracy, measured by

$$\|u - u^E\|_2 = \left\{ \int_{\mathcal{D}} |u - u^E|^2 da \right\}^{1/2}, \tag{21}$$

and execution time measured in central processor seconds. The results were obtained with the CDC Cyber 74 computer at the University of Minnesota. Programs were compiled with the FTN4 (OPT = 2) compiler. Square element grids have been used in all calculations, therefore each grid has been characterized by its corresponding element size h . The full Newton iteration scheme was used to solve the nonlinear equation sets in all calculations.

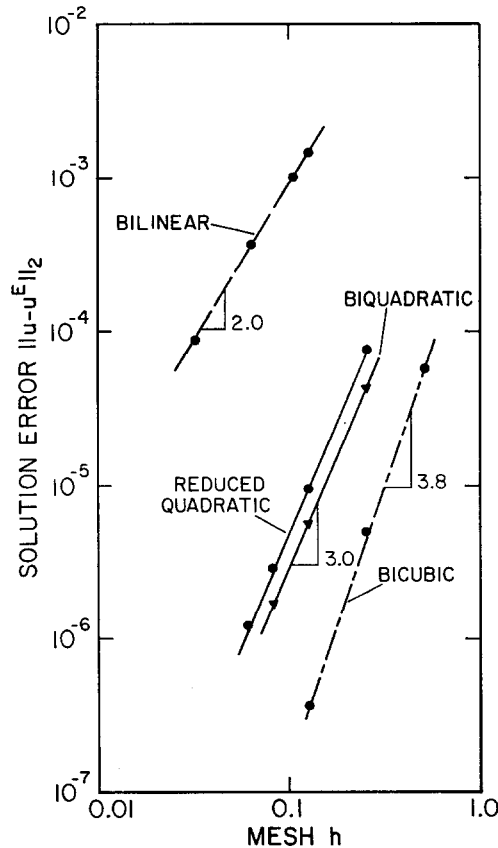


FIG. 5. Convergence of bilinear, reduced quadratic, biquadratic, and Hermite bicubic finite element approximations for the shape of an interface in a square capillary as a function of mesh size h for $\theta_c = 60^\circ$.

Figure 5 shows the accuracy obtained with each finite-element basis as a function of h for $\theta_c = 60^\circ$. As predicted by the analysis for linear equations, the quadratic and Hermite bicubic basis functions gave much improved results over the bilinear elements. If the dependence of the accuracy of the finite-element solution on h is assumed to be of the form

$$\|u - u^E\|_2 = C(\theta_c) h^{r(\theta_c)}, \quad (22)$$

the exponent $r(\theta_c)$ can be evaluated from the slopes of the curves in Fig. 5. With the exception of the Hermite bicubic basis these matched very well with those predicted for linear equations (see Table II).

The relative efficiencies of the four elements for calculating interfaces within a given error tolerance are shown in Fig. 6 again for $\theta_c = 60^\circ$. The high-order accurate elements were much more efficient than the bilinear element. The Hermite bicubic element was the most efficient approximation, especially when extreme accuracy in the solution is desired.

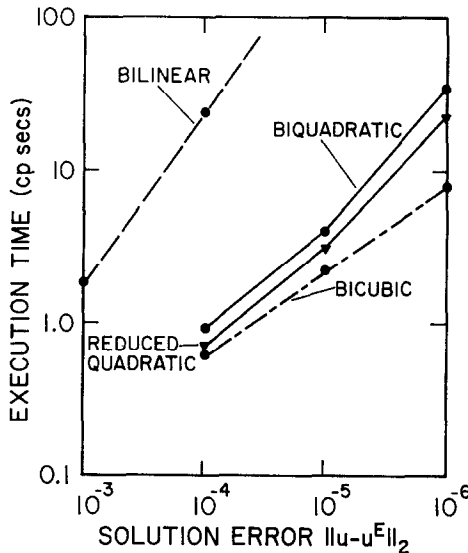


FIG. 6. Execution times (cp sec) as a function of solution error for the four finite-element basis functions with $\theta_c = 60^\circ$.

When the contact angle was lowered to 45° , the rate of convergence of the finite-element solution to the exact solution decreased as shown by the slopes $r(\theta_c)$ in Fig. 7. Again, the Hermite bicubic element gives the most accurate results, but the errors are two orders of magnitude larger than those for $\theta_c = 60^\circ$ and the same grid size. The biquadratic and reduced quadratic elements no longer give the same convergence rates as they did in the $\theta_c = 60^\circ$ calculations. The reduced quadratic elements

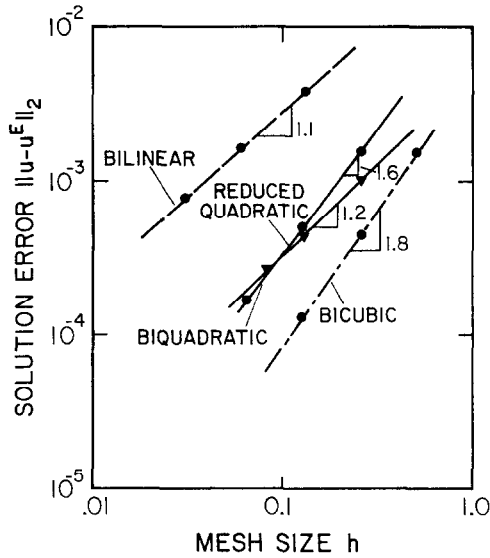


FIG. 7. Convergence of bilinear, reduced quadratic, biquadratic, and Hermite bicubic finite-element approximations for the shape of an interface in a square capillary as a function of mesh size h for $\theta_s = 45^\circ$.

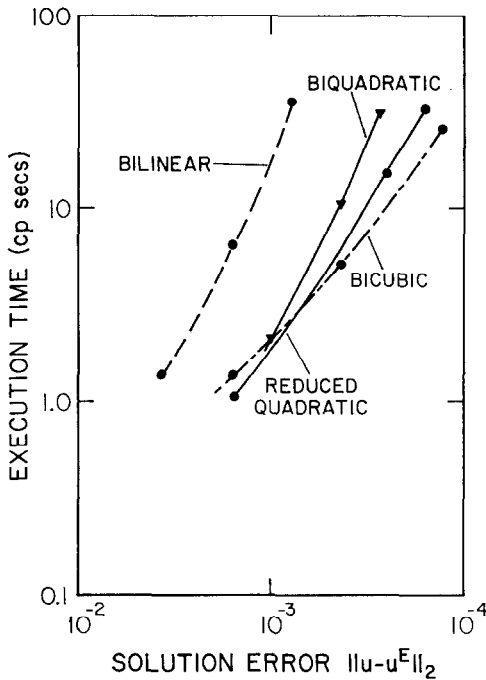


FIG. 8. Execution times (cp sec) as a function of solution error for the four finite-element basis functions with $\theta_s = 45^\circ$.

seemed to give slightly better results for fine grid spacing although the difference is probably not significant.

The error in the finite-element calculations for $\theta_c = 45^\circ$ are plotted as a function of execution time in Fig. 8. The Hermite bicubic element calculations are the most efficient when very accurate solutions are desired. The reduced quadratic element calculations are very efficient, even surpassing the Hermite bicubic calculations for high error tolerances.

The dependence of $\|u - u^E\|_2$ on θ_c for the four elements is plotted in Fig. 9 for $h = 0.125$. The errors in the calculations using the three high-order polynomials all show strong dependence on θ_c , whereas the error in the bilinear calculations is relatively insensitive to θ_c . Such behavior is predicted by finite-element approximation theory [15]. The constant $C(\theta_c)$ in Eq. (22) depends on the true solution which in turn depends on θ_c . The constant for a bilinear approximation is a function of

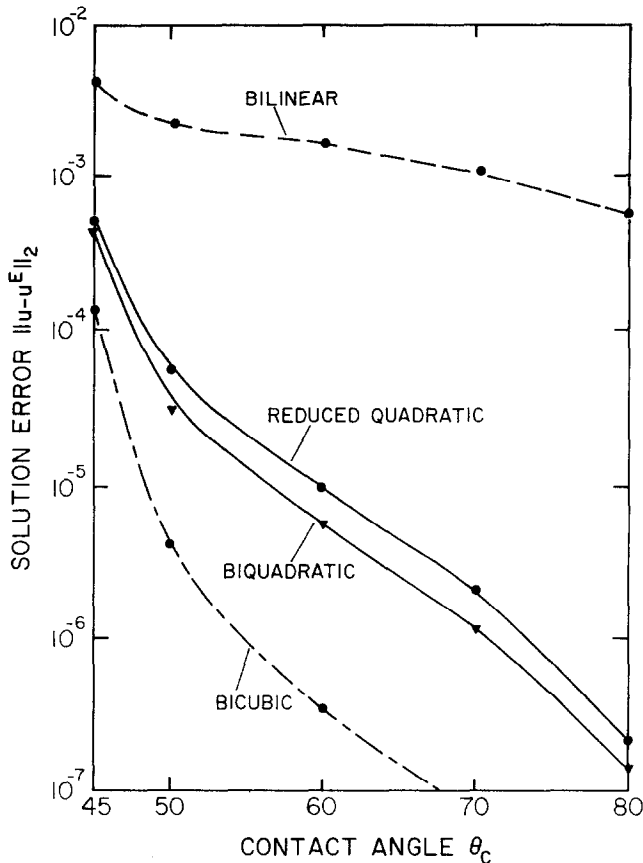


FIG. 9. Error in finite-element approximations as a function of contact angle θ_c for 8×8 element grid ($h = 0.125$).

$\|\nabla u^E\|_2$, whereas the higher-order polynomial approximations depend on the norm of higher-order gradients of the solution. For $\theta_c = 45^\circ$ the gradient of Eq. (7) is singular at $x = 1$ and $y = 1$ as are all higher-order derivatives. These singularities damage the accuracy of the finite-element solutions.

To test the merits of the Galerkin finite-element solution of the capillary problem to other discretization techniques, the reduced quadratic finite-element code was compared to the finite-difference approximation of Concus [10] in which the resulting set of nonlinear equations is solved by successive approximations coupled with the dynamic alternating-direction implicit method of Doss [3, 18] for solving the resulting

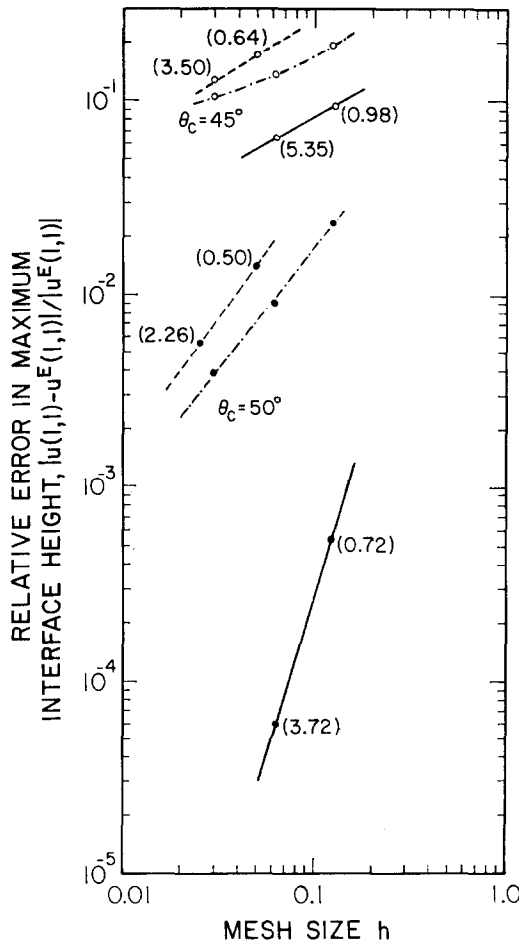


FIG. 10. Convergence of bilinear (---) and reduced quadratic (—) finite-element and finite-difference (-·-) approximations to the maximum interface height in a square capillary for varying mesh size h . Results for $\theta_c = 50^\circ$ and 45° are shown with execution times on the LBL CDC 7600 given in parenthesis.

linear equation set. The tests were run with the CDC 7600 computer at Lawrence Berkeley Laboratory using the before mentioned initial approximation $\{\alpha^{(0)}\}$ and convergence criterion. The relative error in each calculation evaluated at the corner $x = 1$ and $y = 1$ is shown in Fig. 10 as a function of grid size for contact angles of 50° and 45° . The execution times for each calculation are shown in parentheses. The reduced quadratic finite-element solution was more accurate for a given execution time. The finite-difference approximation exhibits a similar convergence rate to the bilinear finite-element approximation also displayed in Fig. 10; this is expected since both techniques reduce to $\mathcal{O}(h^2)$ approximations for linear problems (see [10, 15]).

6. DISCUSSION

The finite-element-Newton methods developed above are well suited to the solution of the capillary equation (3) and the contact angle boundary condition (5), both of which are nonlinear. The reduced quadratic, biquadratic, and Hermite bicubic approximations are all more efficient than the standard bilinear approximation for the model problem considered here. The efficiency of these approximations rests on the small number of elements needed for very accurate solutions; the systems of linear equations resulting from the Newton iteration are of moderate size ($\mathcal{N} < 1000$) and can be solved efficiently by direct factorization using only storage in the computer's central memory. Solutions of this same accuracy constructed from either the bilinear finite-element or finite-difference approximations will involve much larger systems of equations and cannot be efficiently solved by direct methods. As shown above, the high-order accurate finite-element methods are even competitive with finite-difference approximations coupled with very efficient iterative matrix methods.

The finite-element methodology presented here is not limited to geometries as simple as a square. The isoparametric element mappings described in [17] formalize the construction of approximations to irregular boundaries which are consistent with the overall accuracy of the finite-element scheme. The contact-angle boundary condition (5) is incorporated just as above. This is a considerable simplification over finite-difference methods where great care must be taken in constructing an approximation to Eq. (5) consistent with the approximation to the differential equation (4). Isoparametric mappings are employed in [10] for the reduced quadratic finite-element approximation to an interface in a capillary of elliptical cross section.

ACKNOWLEDGMENTS

Part of this work was done while the author was a visitor at Lawrence Berkeley Laboratory. He is indebted to Paul Concus of LBL and L. E. Scriven of University of Minnesota for their comments and suggestions during the course of this study. Thanks are also due to Said Doss of LBL for supplying the results from his finite-difference-DADI technique. This work was partially supported by the University of Minnesota Computer Center.

REFERENCES

1. B. LARKIN, *J. Colloid Interface Sci.* **23** (1967), 350.
2. P. CONCUS, G. H. GOLUB, AND D. P. O'LEARY, *Computing (Arch. Elektron. Rechnen.)* **19** (1978), 321.
3. S. DOSS, Lawrence Berkeley Laboratory Report, LBL-6142, 1977.
4. F. M. ORR, L. E. SCRIVEN, AND A. P. RIVAS, *J. Colloid Interface Sci.* **52** (1975), 602.
5. F. M. ORR, R. A. BROWN, AND L. E. SCRIVEN, *J. Colloid Interface Sci.* **60** (1977), 137.
6. H. D. MITTELMANN, *Computing (Arch. Elektron. Rechnen.)* **18** (1977), 141.
7. N. ALBRIGHT, Lawrence Berkeley Laboratory Report LBL-6136, 1977.
8. W. J. SILLIMAN AND L. E. SCRIVEN, *J. Colloid Interface Sci.*, to appear.
9. R. A. BROWN, F. M. ORR, AND L. E. SCRIVEN, *J. Colloid Interface Sci.*, to appear.
10. R. A. BROWN, Lawrence Berkeley Laboratory Report LBL-7291, 1977.
11. P. CONCUS, *J. Computational Phys.* **21** (1967), 340.
12. J. DOUGLAS, JR. AND T. DUPONT, *Math. Comp.* **29** (1975), 689.
13. G. J. FIX, B. NETA, *Comput. Math. Appl.* **3** (1977), 287.
14. P. CONCUS, R. FINN, *Acta Math.* **132** (1974), 179.
15. G. STRANG AND G. J. FIX, "An Analysis of the Finite Element Method," Prentice-Hall, Englewood Cliffs, N. J., 1973.
16. W. C. RHEINBOLT, "Methods for Solving Systems of Nonlinear Equations," Society for Industrial and Applied Mathematics, Philadelphia, 1974.
17. K. J. BATHE AND E. L. WILSON, "Numerical Methods in Finite Element Analysis," Prentice-Hall, Englewood Cliffs, N. J., 1976.
18. S. DOSS, private communication.